Ministry of Higher Education
and Scientific Research

Journal of Kufa for Chemical Sciences

A refereed

Research Journal Chemical Sciences
Vol.2 No.9 Year 2022
ISSN 2077-2351

Adsorption of Methylene Blue and Safranine Using Activated Carbon of Cinnamon Plant Surface.

Delfaa Slman Gassed , Ali Abdulrazzaq Abdulwahid and Ali A. A. Al-Riyahee

delfaaslman2018@gmail.com , *ali.abdulwahid@uobasrah.edu.iq* , *ali.abdulzahraa@uobasrah.edu.iq*

Chemistry Department/College of Science/University of Basrah.

Abstract

Cinnamon plant Activated Carbon (C/AC) was prepared by chemical and thermal activation. The adsorption behaviour of (C/AC) in aqueous Methylene blue (MB) and Safranine (S) dyes was investigated and characterized by XRD, TEM and FESEM. The possible mechanism of the adsorption of (MB) and (S) dyes on the (C/AC) surface was studied. The influence of various adsorption control parameters like the initial dye concentration, pH, contact time, and temperature was studied. The data confirmed a high removal of (MB) and (S) at pH=11. The experimental data were fitted to Langmuir and Freundlich isotherms to examine the adsorption mechanism. The adsorption data reveal (MB) with the maximum capacity of (294.11) mg/g and (S) with the capacity of (285.714) mg/g. The kinetic data for different initial dye concentration were computed using pseudo-first order, pseudo-second order, and intraparticle diffusion model. Thermodynamic parameters includes enthalpy (ΔH), entropy (ΔS), free energy (ΔG), and activation energy (E_a) of the adsorption process were calculated and used to interpret the results, and revealed that the adsorption systems were a spontaneous and endothermic process for adsorption of MB and S dyes onto the adsorbent surface. Also, low activation energy values (E_a<40 kJ/mol) were characteristics of the physisorption mechanism and diffusion-controlled process.

Key words: Cinnamon plant, Active carbon, Adsorption of dyes, Methylene blue, Safranine.

1.Introduction

Dyes are widely used in several industrial application such as in textiles, plastics, printing, rubber, cosmetics, paper and pulp, leather, and pharmaceutical [1,2]. After a dying process, a large amount of dye wastewater is generated and released into the environment [3]. Unfortunately, about 12% of synthetic dyes are lost during manufacturing and processing, and approximately 20% of them enter industrial wastewater [4]. Dyes wastewater seriously threat the ecological system and human health because many of the dye wastewater are difficult to treat and are very strongly oncogenic [5-7]. These dyes have a statable, symmetric, and complex aromatic structure that make them nondegradable [8].

In general, the dye is toxic and hazardous chemicals in the environment, particularly in the water bodies and biosphere. In addition the dye can cause dysfunction of the kidneys, reproductive system, liver, brain, and nervous system of human beings [9]. Approximately, 100,000 different types of dyestuffs are available on the global market but the annual production rate is about 7×10^5 t [10]. Methylene blue is cationic dye with heterocyclic aromatic chemical compound ($C_{16}H_{18}N_3SC$) which is commonly used for dyeing of cotton, wool and silk. About 40% 0f the synthetic dyes like methylene blue and Safranine are toxic, mutagenic, and carcinogenic compounds that remained in industrial effluent and can cause sever public and environmental health problems [11].

Generally, conventional wastewater treatment plants are not effective for the removal of dyes from textile industrial wastewater. However, advanced wastewater treatment for dyes removal from textile industrial wastewater are very effective and efficient. The most applicable advanced wastewater treatments are chemical precipitation, nanofiltration, advanced oxidation process, ion exchange, reverse osmosis, membrane separation, electro-coagulation, and electrodialysis. However, these technologies are a very expensive and not sustainable mechanism for wastewater treatment in every sector, especially in developing countries [12]. In addition these methods required high energy, chemical, operational and capital inputs, and advanced technologies. Among advanced treatment methods, adsorption has been found to be good treatment technology for dye removal [13,14], and the researchers have relied on many ideas and new materials used as adsorbent surfaces [15,16].

Fundamentally, adsorption treatment technology is flexible, simple for design, relative ease of operation, cost-effective, high efficiency, recyclability, and environmentally friendly [12]. The technical and economical disadvantages have resulted in using bio-sorption methods that has been found to be efficient and cost-effective. The use of activated carbon biosorbent not only serves to control pollution but also reduces agricultural waste generation. Various agricultural waste biomaterials were used for adsorption process such as rambutan seed, Rambutan seeds activated carbon (RSAC) was prepared using potassium hydroxide (KOH) activation and carbon dioxide (CO_2) gasification methods, RSAC used for the removal of MG dye [17], spent tea leaves [18], pomelo peel [19], sugar beet pulp[20] sugar beet pulp based activated carbon was prepared by using phosphoric acid as activating agent for adsorption of methylene blue, and rice husk[21] concluded from this study that porous bio-char and activated carbon could be prepared in normal environmental conditions instead of inert media. This study shows a method and possibility of activated carbon from agro-waste, and it could be scaled up for commercial production. The remarkable adsorption characteristics of activated carbon are that it contains small, low-volume pores that increase the surface area available for adsorption or chemical reaction [22].

Cinnamon is a spice obtained from the inner bark of several tree species from the genus Cinnamomum. Cinnamon is used mainly as an aromatic condiment and flavouring additive in a wide variety of cuisines, sweet and savoury dishes, tea and traditional foods. The aroma and flavour of Cinnamon derive from its essential oil and principal component, cinnamaldehyde, as well as numerous other constituents including eugenol. Cinnamon is the name for several species of trees and the commercial spices products that some of them produce. All are members of the genus Cinnamomum in the family Lauraceae. Only a few Cinnamomum species are grown commercially for spice [23].

2. Material and Methods

Preparation of Adsorbent and Adsorbate. The dried ground Cinnamon was subjected to chemical activation with 20.4 ml of 1N H_3PO_4 were measured into a crucible containing 5g from laboratory ground Cinnamon carefully measured and stirring for 30 minutes at room temperature. The sample was oven dried for 24 hours at 105^0C and then allowed to cool.

After cooling the sample was activated in the furnace for 1 hour at 700^0C. This was followed by soaking the activated carbon in 0.1N HCl, and stirred for 30 minutes then allowed to stand for 24 hours and washing with distilled water until the pH is in the range of 6-7, all of that to remove the residual acid from its pores.

After that the sample was oven dried for 24 hours at 105^0C and cooled, crushed, and sieved (by using 75- micron sieve). Methylene blue and Safranine were purchased from (Sigma-Aldrich) and used to prepare adsorbate solution. The stock solution of the dyes of 1000 ppm was prepared using de-ionized distilled water.

3. Experimental

A series of dye solutions were prepared by adjusting the pH over a range of (3-5-7-9-11) by using 0.1N HCl and 0.1N NaOH solution to evaluate the role of pH on adsorption of Methylene blue and Safranine dyes onto (Cinnamon/Active Carbon) or (C/AC). The experiment was carried out using 100ml of the aqueous MB and S dyes at concentrations 200ppm. It was treated with 0.25g of (C/AC) and shaken in bench top incubator cum orbital shaker at a constant speed of 200rpm for a time period of 3hours.

Residual dye concentration was recorded using a double beam UV/vis spectrophotometer (Model: T80 (EMC-LAB) / PG instruments, England) at 668nm for MB and 525nm for S for which the molecular structure is shown in Fig.1 and 2. The equilibrium amount of dye adsorbed on (C/AC) was calculated by equation 1, and the removal efficiency of the dye in percentage was calculated by equation 2 as listed in Table1.

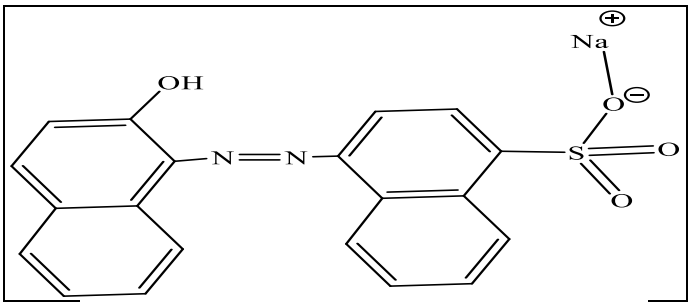

Figure (1) Methylene Blue Dye Structure.

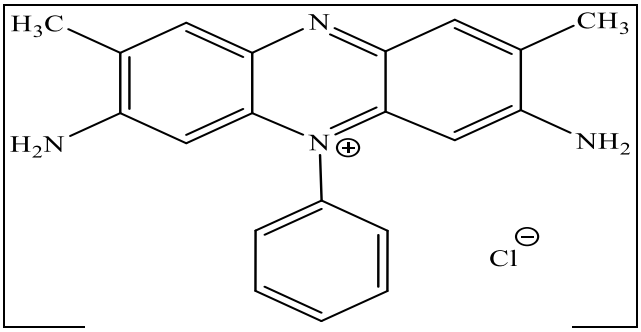

Figure (2) Safranine Dye Structure.

1.3 ***Adsorption Isotherms.*** The adsorbate-adsorbent interaction at equilibrium was found by fitting the experimental data in Langmuir, and Freundlich 3, and 5 respectively, as summarized in Table 1.

2**.3** ***Kinetic Studies***. The equation 6, 7, and 8 shown in Table 1 were used to examine the reaction kinetics for a specific contact time, t (5, 15, 30, 45, 60, 80, 120, and 180 min.) using 0.25g of (C/AC) with 200 ppm MB and S dye solutions, at room temperature.

3.3 ***Thermodynamic Studies***. The thermodynamic nature of adsorption of MB and S onto (C/AC) was studied using Gibbs and Van't Hoof equations 9, and 10 as given in Table 1.

Table 1: Equation of adsorption functions

Equation number	Adsorption function	Equation
1.	Equilibrium amount of dye adsorption	$qe = (C_0 - C_e/M) \times V$
2.	Removal efficiency , %	$((C_0 - C_e)/(C_0)) \times 100$

Where C_0 is the initial dye concentration, C_e is the final dye concentration at equilibrium, *V* is the operating volume of the solution, and *M* is the mass of adsorbent.

3.	Langmuir isotherm	$^1/_{q_e} = ^1/_{q_m} + ^1/_{K_L C_e q_m}$
4.	Dimensional separator factor	$R_L = ^1/_{1 + K_L \times C_e}$
5.	Freundlich isotherm	$\log q_e = \log K_F + (^1/_n) \log C_e$

Where q_e is the amount of dye adsorbed per g, q_m is the monolayer adsorption capacity, K_L is Langmuir adsorption constant, *n* is Freundlich constant.

Kinetic studies

6.	Pseudo-first order equation	$\log(q_e - q_t) = \log q_e - k_1 \, ^t/_{2.303}$
7.	Pseudo-second order equation	$t/q_t = (1/k_2 q_e^{\,2}) + t/q_e$
8.	Intraparticle diffusion	$q_t = k_i t^{1/2} + C$

Where q_e is the amount of dye adsorbed at equilibrium, q_t is the amount of dye adsorbed at any time t, k_1 is the pseudofirst order rate constant in s^{-1} , k_2 is the pseudosecond order rate constant, k_i is the intraparticle diffusion rate constant, and *C* is the intercept.

Thermodynamic studies.

9.	Gibbs equation	$\Delta G^0 = \Delta H^0 - T\Delta S^0$
10.	Van't Hoff equation	$\Delta G^0 = -RT \ln K_e$

Where K_e is the equilibrium constant, ΔG^0 is Gibbs free energy change, ΔH^0 is the change in enthalpy of adsorption, ΔS^0 is entropy change, and *T* is the operating temperature.

4.**3** ***Characterization of (C/AC)***. The physical characteristics of (C/AC) such as the surface morphology of (C/AC) was characterized by Field Emission Scanning Electron Microscopy (FESEM) using the (FEI NOVA Nano SEM 450) model. Figure (3) the (SEM) image of the (C/AC) sample obviously shows the surface morphology with an irregular texture and high surface roughness and different levels of porosity, which provides possible sites for adsorption of the dyes. The surface roughness and the macropores which are important factors for the dye

adsorption were responsible for the high surface area making the (C/AC) a good adsorbent [24].

(C/AC) also characterized by X-Ray Diffraction using (Rigaku X-Ray Powder Diffraction Diffractometer). Figure (4) shows the XRD pattern of (C/AC), the broad peaks at round 25^0 and 43^0 due to the hexagonal graphite structures (002) and (100). The d_{002} value of (C/AC) calculated using Bragg's equation ($d = n\,\lambda/2\sin\theta$) by assumed n=1, and $\lambda\ for\ coper = 0.154$nm, the result was (0.371 nm) which is higher than that in graphite (d_{002} = 0.335 nm). Indicating that (C/AC) had more randomly oriented graphitic carbon layers [25,26].

Transmission Electron Microscopy (TEM) analysis was also performed by using (CM 120, 100Kv, Philips) model. As shown in Figure (5) which revealed a complete porous carbon architecture. The existence of these pores is attributed to the H_3PO_4 activation process adopted in synthesizing of (C/AC) [27,28].

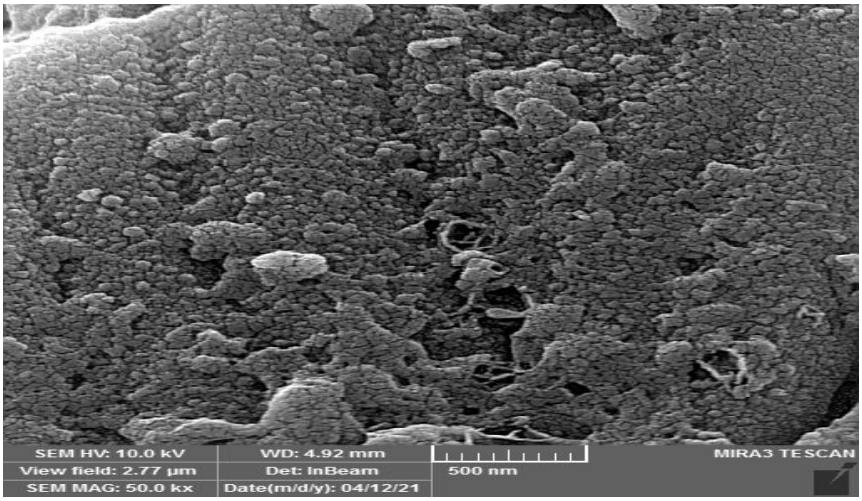

Figure (3) SEM

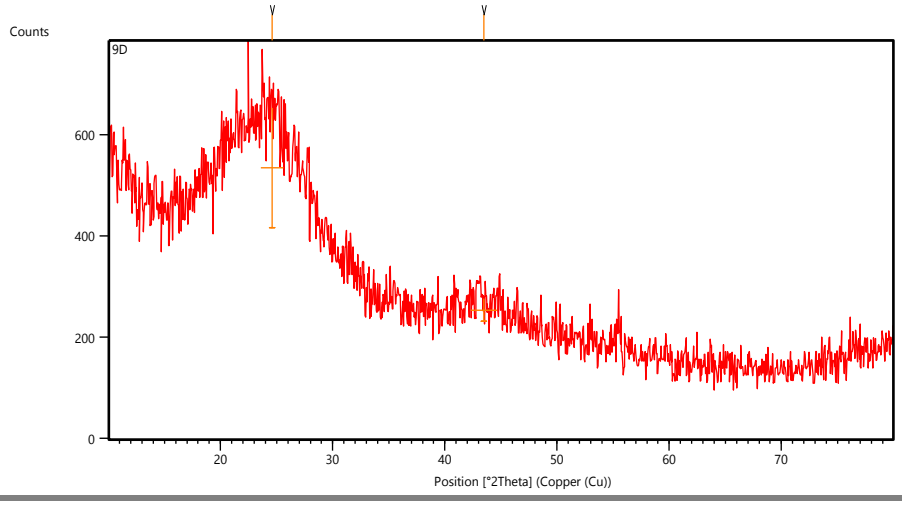

Figure (4) XRD

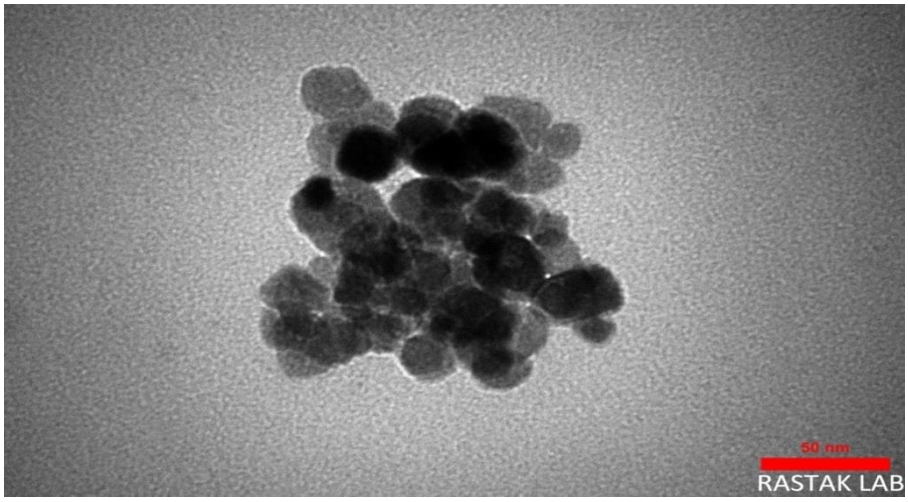

Figure (5) TEM

5.3 ***Effect of pH on Dyes Removal.*** The pH of the solution influences the surface of the adsorbent and ionization characteristics of the adsorbate [29]. From the experimental data, it is found that the removal efficiency of MB and S dyes increased with increasing of pH from (3 to 11) as shown in Figure (6) and Figure (7) respectively. Maximum adsorption for MB and S was observed at pH=11 and it was (221.850 mg/g) for MB and (177.203 mg/g) for S. The increase in the adsorption efficiency in the alkaline medium is due to the strong hydrostatic interactions between the adsorbent molecules and the dyes. On the other hand, the increase in the adsorption efficiency depend on the competition between hydrogen ions H^+ and the dye ions to be adsorbed from their aqueous solution on the active sites of the adsorbent surfaces, in the lower value of pH (2-6) (acidic medium) the hydrogen ions H^+ concentration is increase and the competition between them and the dye ions to be adsorbed on the active side of the adsorbent surface increase that leads to decrease in the adsorption efficiency. The increasing of pH values (alkaline medium), the hydrogen ion H^+ concentration decreases and thus the competition between hydrogen ion H^+ and the dye ions to be adsorbed on the active site located on the surface of the adsorbent is decrease, which leads to an increase in the adsorption efficiency directly until reaching for the optimum pH value [30,31].

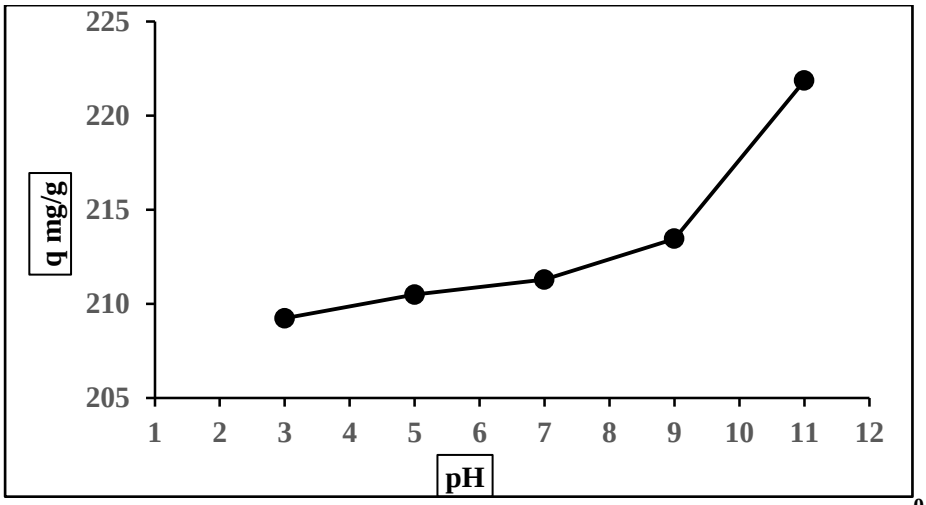

Figure (6) Effect of pH (3 to 11) in adsorption of MB on (C/AC) at 25^{0}C

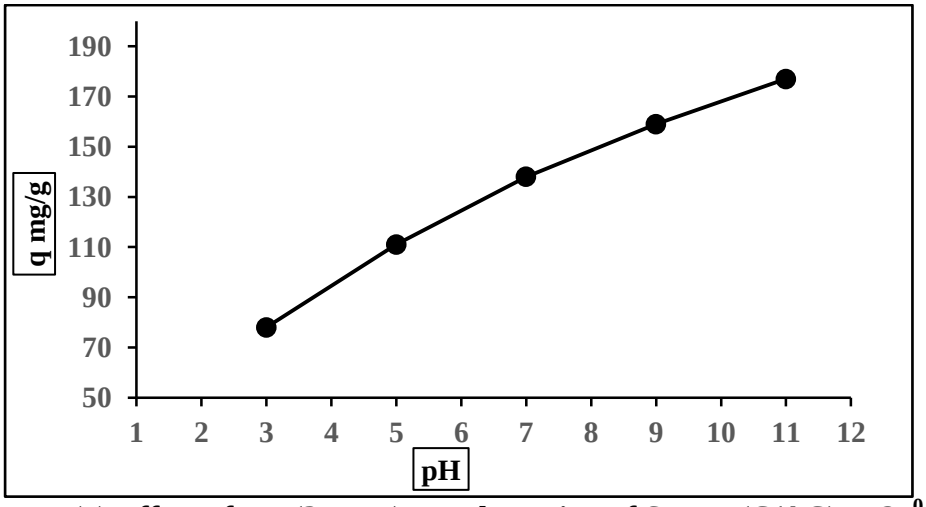

Figure (7) Effect of pH (3 to 11) on adsorption of S onto (C/AC) at 25^{0}C

6.**3** ***Effect of Contact Time and Temperatures on dyes adsorption***. The effect of contact time between the adsorbate and adsorbent is one of the most important parameters in the adsorption process since it is important to estimate the equilibrium contact time to foretell the performance and feasibility of an adsorption for a process[32].

The effect of contact time on the adsorption of MB and S onto (C/AC) were presented in Figures (8) and (9), at the initial concentration of adsorbent and optimum pH=11 in three different temperatures (25, 40, 60)^{0}C. As shown in both Figures (8) and (9) the adsorption had increased rapidly from 5-180 min for MB. While the adsorption of S had increased rapidly from 5-120 min and then the equilibrium was achieved within 180min for MB and 120min for S.

Generally, the trend was observed for dyes adsorption onto (C/AC) was the same, it is clear that the extent of adsorption was rapid in the initial stages, because of the availability of a wide number of adsorption active sites on the adsorbent

surface and becomes slow in later stages due to a reduction in the number of adsorption active sites on the surface of the adsorbent until equilibrium was achieved. Also, the Figures showed that the adsorption capacity of prepared adsorbent surface (C/AC) for MB and S dyes increased with temperature from 25^0C to 60^0C. This may be ascribed that with an increase in temperature there was an increase in the mobility of the large dye ion. An increasing number of molecules also acquire sufficient energy to undergo an interaction with active sites at the surface [33].

Besides that, the equilibrium capacity of the adsorbent for a specific adsorbate can be affected by temperature change [34].

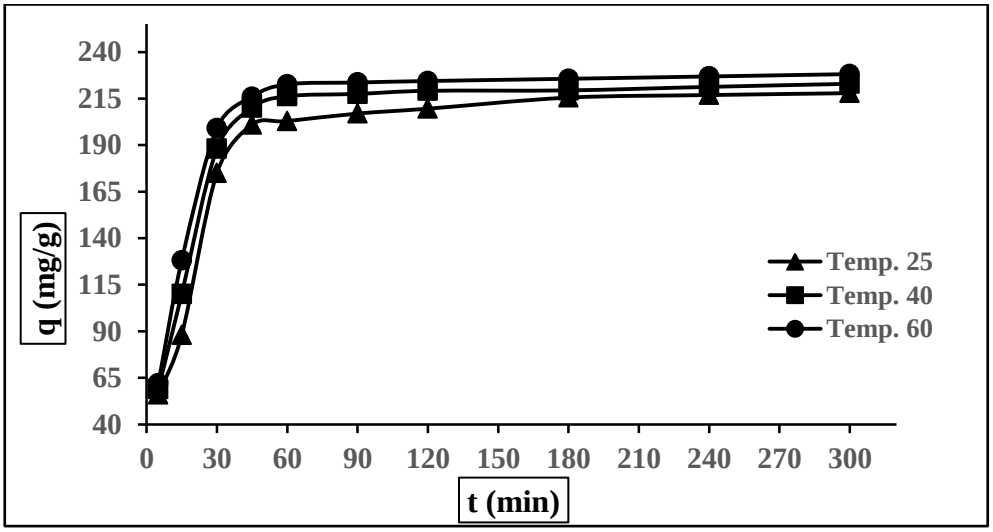

Figure (8) Effect of Time and Temperature on adsorption of MB dye onto (C/AC) at (25,40,60)^{0}C, pH=11, 200ppm and 0.25g

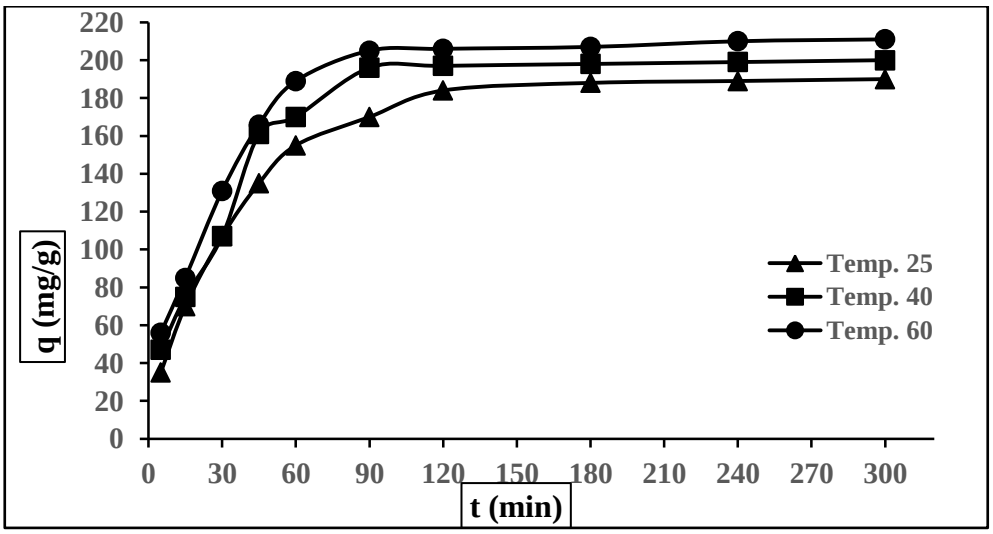

Figure (9) Effect of Time and Temperature on adsorption of S dye onto (C/AC) at (25,40,60)^{0}C, pH=11, 200ppm and 0.25g

7.3 ***Isotherm Studies.*** The study on adsorption isotherm is very important in describing the adsorption characteristics for a solid-liquid adsorption system [35]. Figure (10) and Figure (11) gives the Langmuir plot ($C_e$vs.C_e /q_e) for MB and S dye adsorption and isotherm constant q_m and K_L are from the slope and intercept, respectively.

Langmuir isotherm assumes adsorption at homogeneous sites on the adsorbent thus forming a saturated monolayer of the dye inside the pores [36].

The dimensionless separation factor R_L if ($0 < R_L < 1$ favourable, $R_L > 1$ unfavourable, $R_L = 0$ irreversible) for the adsorption of MB was (R_L= 0.045) and for S was ($R_{L=}$ 0.079) were assumed the adsorption was favourable.

Freundlich isotherm describes heterogeneity and multilayer adsorption process. Figure (12) and (13) shows the Freundlich plot ($\ln q_e$ vs. $\ln C_e$) for adsorption of MB and S dyes on (C/AC) where the slope and intercept give the value of Freundlich constant *n* and K_F, respectively.

Freundlich constant ($1/n < 1$), ($1/n$ =0.1737) for MB and ($1/n$ =0.2070) for S dyes proves the feasibility of multilayer adsorption of the dyes onto (C/AC) [37]. During multilayer adsorption of MB and S dyes, the energy of interaction between the adsorbate and the adsorbent is strongest in the first layer and gradually decreases for the subsequent layers. The adsorption of MB and S dyes on (C/AC) displays best fit in Freundlich plot (R^2_{max} = 0:9997) for MB and (R^2_{max} = 0.9998) for S dye.

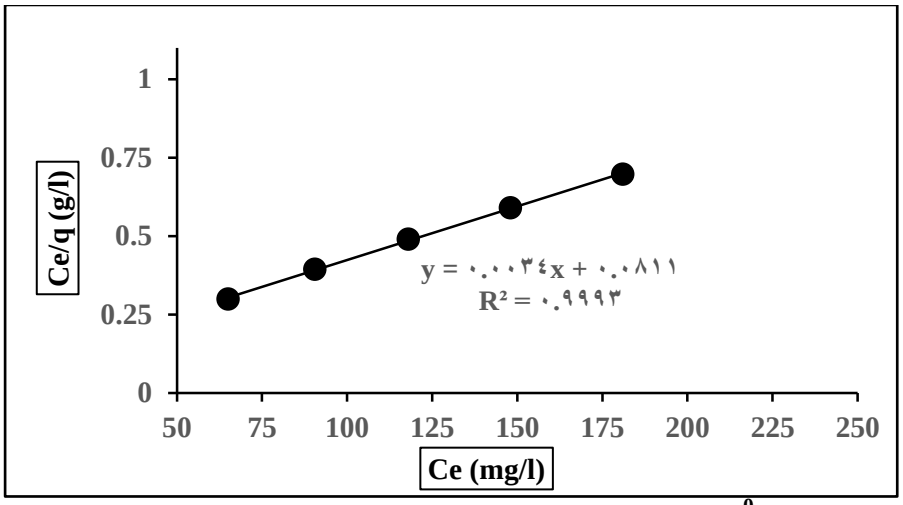

Figure (10) Langmuir plot of MB adsorption onto (C/AC) at (25)^{0}C, pH=11, and 0.25g, 200ppm

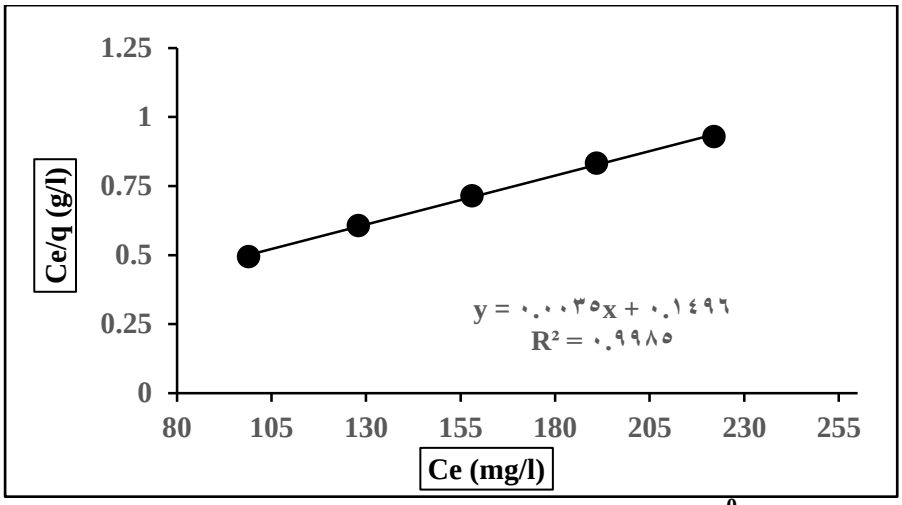

Figure (11) Langmuir plot of S adsorption onto (C/AC) at (25)^{0}C, pH=11, and 0.25g, 200ppm

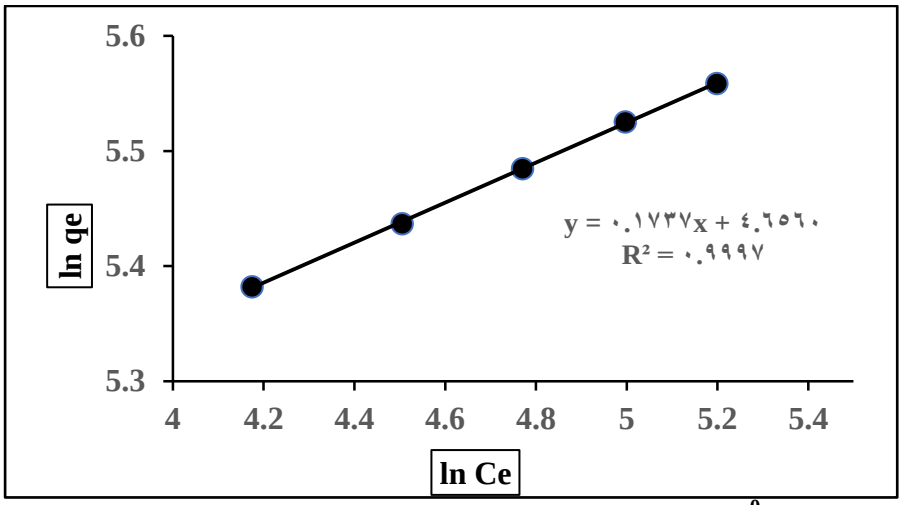

Figure (12) Freundlich plot of MB adsorption onto (C/AC) at (25)^{0}C, pH=11, and 0.25g, 200ppm

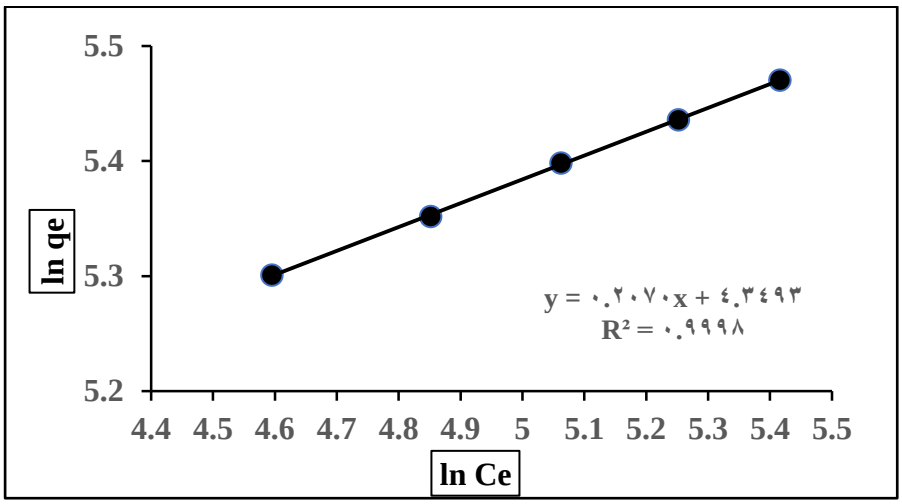

Figure (13) Freundlich plot of S adsorption onto (C/AC) at (25)^{0}C, pH=11, and 0.25g, 200ppm

Table 2: Langmuir isotherm parameters for MB and S adsorption onto (C/AC) at (25)^{0}C, pH=11, and 0.25g, 200ppm.

Safranine				Methylene blue			
R^2	R_L	K_L(L/mg)	q_{max}(mg/g)	R^2	R_L	K_L(L/mg)	q_{max}(mg/g)
0.9985	0.079	0.0233	285.714	0.9993	0.045	0.04192	294.1175

Table 3: Freundlich isotherm parameters for MB and S adsorption onto (C/AC) at (25)^{0}C, pH=11, and 0.25g, 200ppm.

Safranine			Methylene blue		
R^2	1/n	K_F(L/mg)	R^2	1/n	K_F(L/mg)
0.9998	0.2074	77.4242	0.9997	0.1737	105.2143

8.**3** ***Kinetic Studies*****.** Kinetic models such as pseudo-first order, pseudo-second order, and intraparticle diffusion models were used to interpret the experimented data [38]. The plot (ln ($q_e - q_t$) vs. t) for linearized Lagergren pseudo-first order equation for MB and S is given by Figures (14) and (15). The values of (- K_1) and q_1 were calculated from the slope and intercept respectively, and R^2 is listed in Table (4). The straight lines in the pseudo-first order plot for MB and S dyes imply the feasibility of pseudo-first order kinetics. Further, the values of coefficient of determination, $R^2 > 0.9$, for MB and S dyes, adsorption confirm the best fit [39]. However, pseudo-second order plot (t/q_t vs. t) shown in Figures (16) and (17), did not indicate a good compliance for MB and S dyes adsorption and thus proves the no proximity of the model against the examined data. The intraparticle diffusion mechanism ascribes to the travelling of dye molecules from the bulk of the solution to the solid adsorbent. This mechanism can be understood from the plot (q_t vs. $t^{1/2}$) for MB and S dyes adsorption as displayed in Figures (18) and (19). The plot indicates a linear regression for MB and S dyes and skips away from the origin. This infers that intraparticle diffusion mechanism onto (C/AC) was not the rate-determining step and not the overall step controlling adsorption process [40].

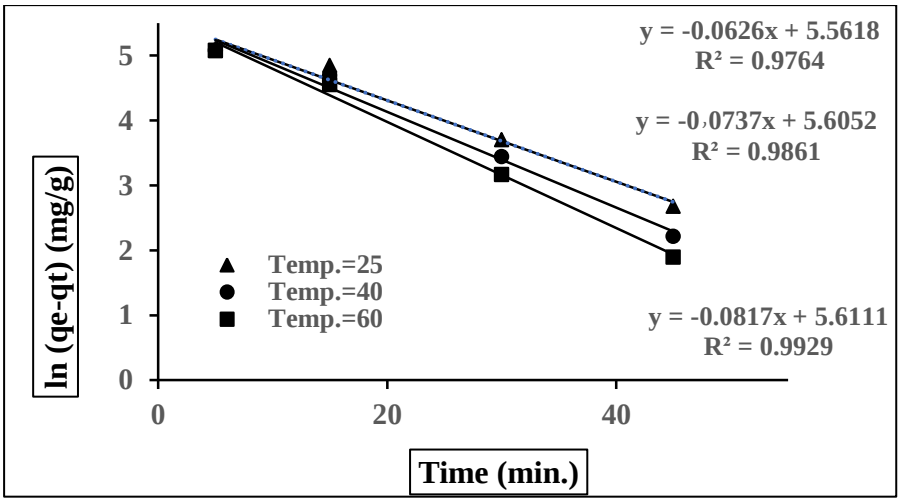

Figure (14) Pseudo-first order plot of MB adsorption onto (C/AC) at (25,40,60)^{0}C, pH=11, 200ppm and 0.25g, 200ppm.

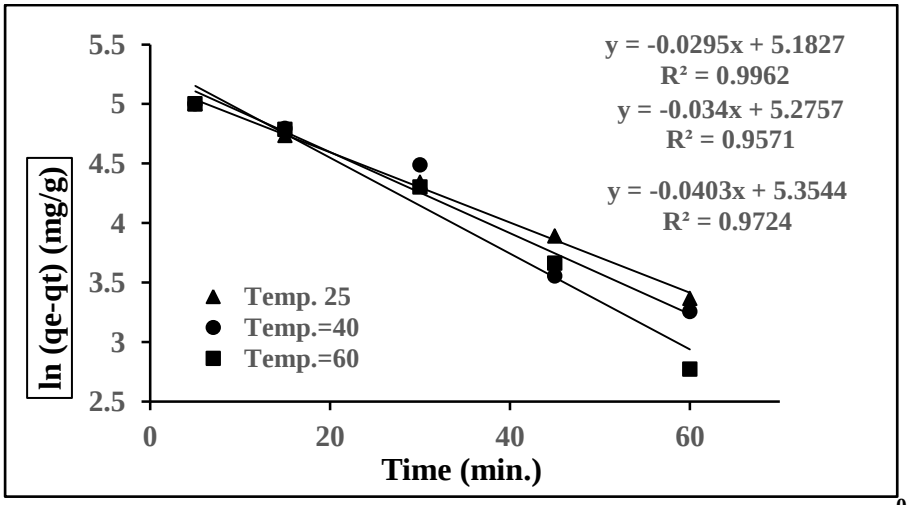

Figure (15) Pseudo-first order plot of S adsorption onto (C/AC) at (25,40,60)^{0}C, pH=11, 200ppm and 0.25g 200ppm.

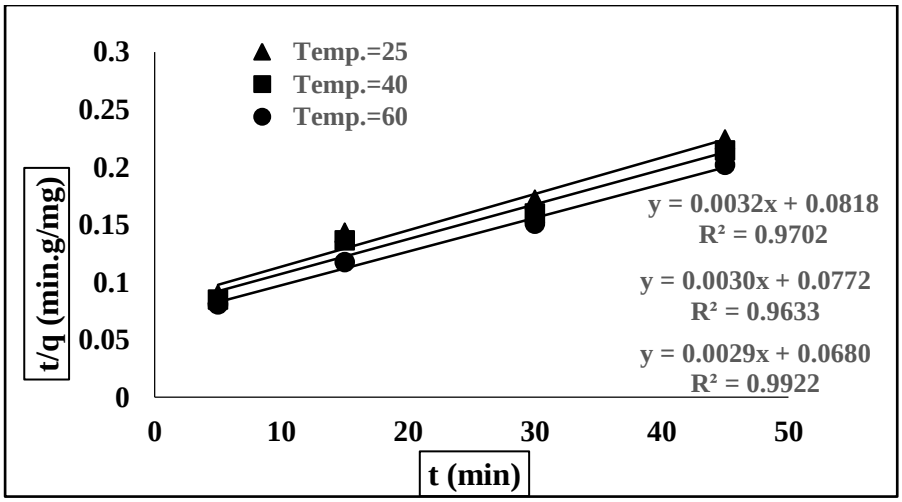

Figure (16) Pseudo-second order plot of MB adsorption onto (C/AC) at (25,40,60)^{0}C, pH=11, 200ppm and 0.25g

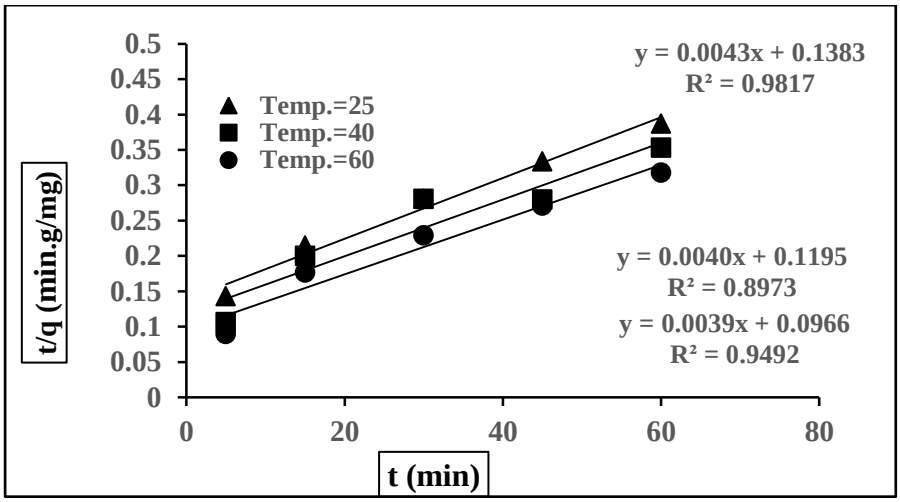

Figure (17) Pseudo-second order plot of S adsorption onto (C/AC) at (25,40,60)^{0}C, pH=11, 200ppm and 0.25g

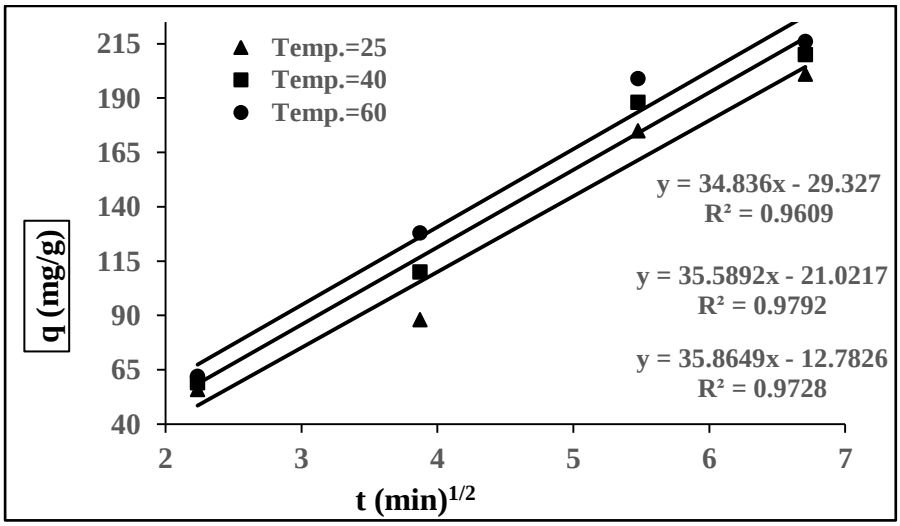

Figure (18) Intraparticle diffusion plot of MB adsorption onto (C/AC) at (25,40,60)^{0}C, pH=11, 200ppm and 0.25g

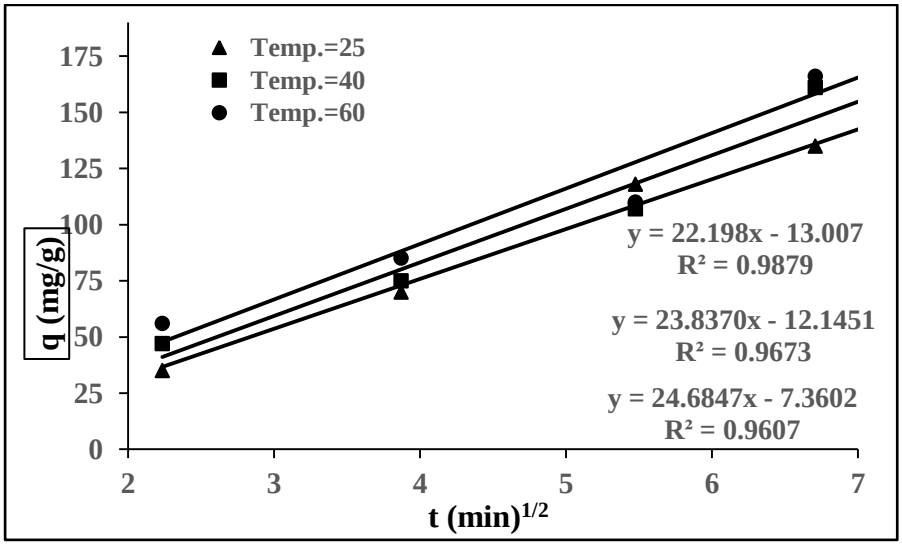

Figure (19) Intraparticle diffusion plot of S adsorption onto (C/AC) at (25,40,60)^{0}C, pH=11, 200ppm and 0.25g

Table 4: Pseudo-first order parameters for MB and S adsorption onto (C/AC) , pH=11, 200ppm, (25,40,60) ^{0}C

Safranine			Methylene blue			Temperature °C
R_1^2	q_1(mg/g)	K_1(min^{-1})	R_1^2	q_1(mg/g)	K_1(min^{-1})	
0.9962	178.1632	0.0295	0.9764	260.2909	0.0626	25
0.9571	195.5273	0.0341	0.9861	271.8362	0.0737	40
0.9724	211.5371	0.0403	0.9929	273.4448	0.0817	60

Table 5: Pseudo-second order parameters for MB and S adsorption onto (C/AC) , pH=11, 200ppm, (25,40,60) ^{0}C

Safranine			Methylene blue			Temperature ^{0}C
R_2^2	q_2 (mg/g)	K_2(g.mg^{-1}.min^{-1})	R_2^2	q_2 (mg/g)	K_2(g.mg^{-1}.min^{-1})	
0.9817	232.5581	0.0001336	0.9702	312.500	0.000125	25
0.8973	250	0.0001338	0.9633	333.3333	0.000116	40
0.9492	256.4103	0.000157	0.9922	344.8276	0.000123	60

Table 6: Intraparticle diffusion parameters for MB and S adsorption onto (C/AC) , pH=11, 200ppm, (25,40,60) ^{0}C

Safranine			Methylene blue			Temperature ^{0}C
R^2	C(mg/g)	K_P(mg.g^{-1}min$^{-1/2}$)	R^2	C(mg/g)	K_P(mg.g^{-1}min$^{-1/2}$)	
0.9879	-13.007	22.1981	0.9609	-29.327	34.8360	25
0.9673	-12.145	23.8373	0.9792	-21.021	35.5892	40
0.9607	17.360	24.6851	0.9728	-12.782	35.8649	60

9.3 ***Thermodynamic Studies.*** The values of ΔG, ΔH, and ΔS were calculated for the adsorption of MB and S dyes on (C/AC) as listed in Table (7). ΔH and ΔS were obtained from the slope and intercept of the linear plot of Van't Hoff of (ln K_{eq} vs. 1/T) as shown in Figures (20) and (21). These parameters allow for the determination of whether the process is favorable from thermodynamic standpoint, the system's spontaneity, and whether the adsorption process occurs with adsorption or release of energy [41].

The positive values of ΔH for adsorption of MB and S onto (C/AC) also prove the endothermic nature of the process [42,43]. The positive values of ΔS indicate increase in randomness at the carbon-dye interface during the adsorption

of dyes onto (C/AC), this could be possible due to the increase in mobility of adsorbate molecules present in the solution with an increase in temperature [44], and the adsorption systems were spontaneous revealed that from negative values of ΔG.

Also, the E_a was calculated from the plots of (ln K vs. 1/T) as shown in Figures (22) and (23) and the slope of the straight line gives the E_a values, the activation energy E_a gives indicates whether the adsorption mechanism is primarily physical or chemical [45]. Generally low activation energy (less than 40 KJ mol^{-1}) for adsorption of MB and S dyes onto (C/AC) are characteristic for physisorption [46].

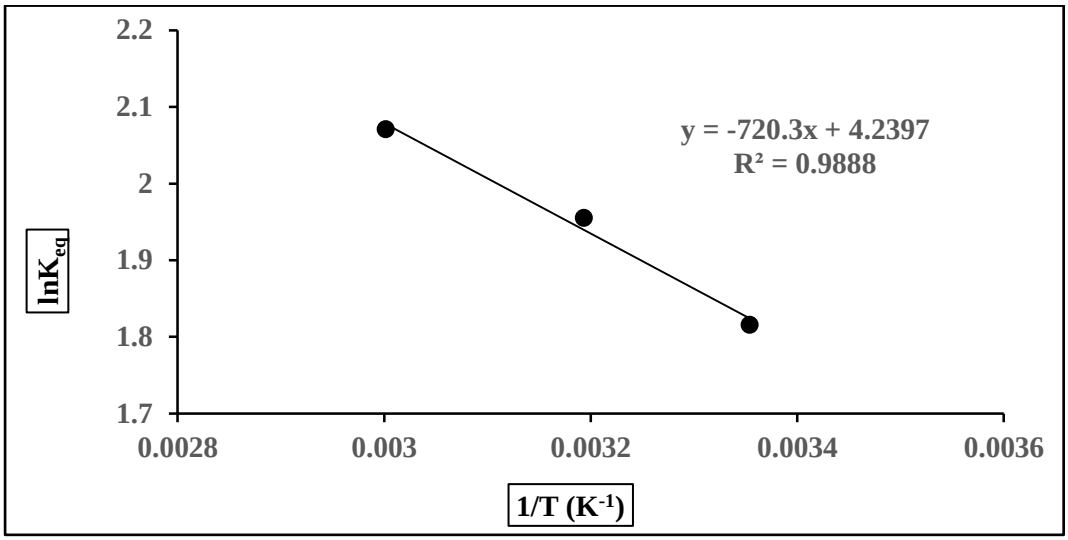

Figure (20): Van't Hoff plot model for MB adsorption onto (C/AC) , pH=11, 200ppm, (25,40,60) ^{0}C

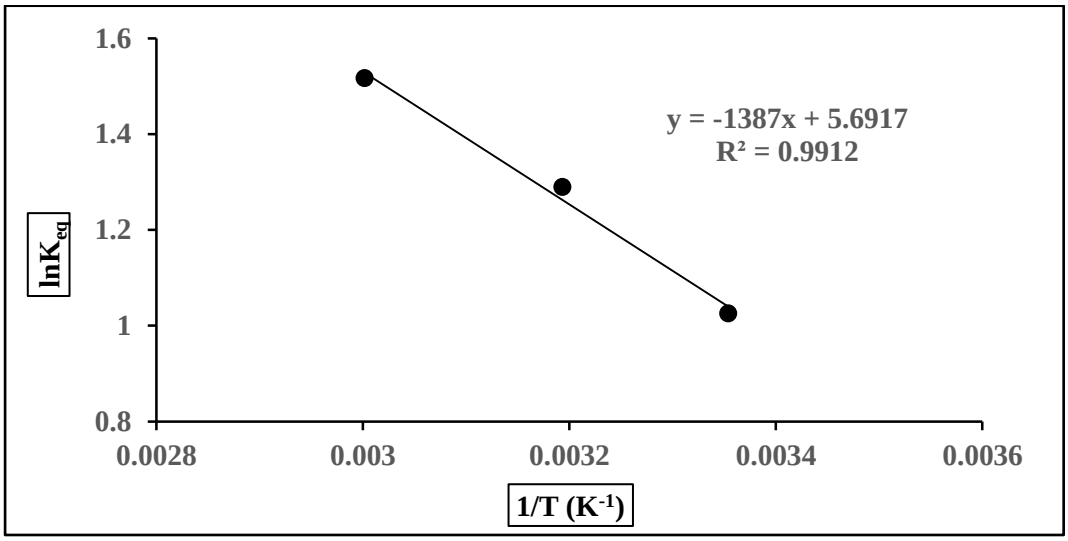

Figure (21): Van't Hoff plot model for S adsorption onto (C/AC), pH=11, 200ppm, (25,40,60) ^{0}C

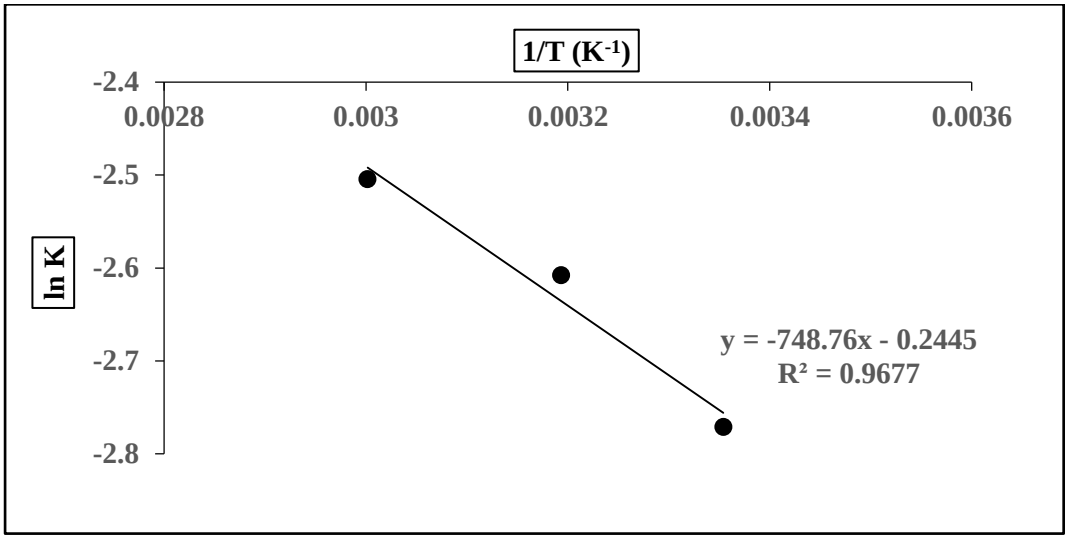

Figure (22): Plot (ln K vs. 1/T) for MB adsorption onto (C/AC) , pH=11, 200ppm, (25,40,60) ^{0}C

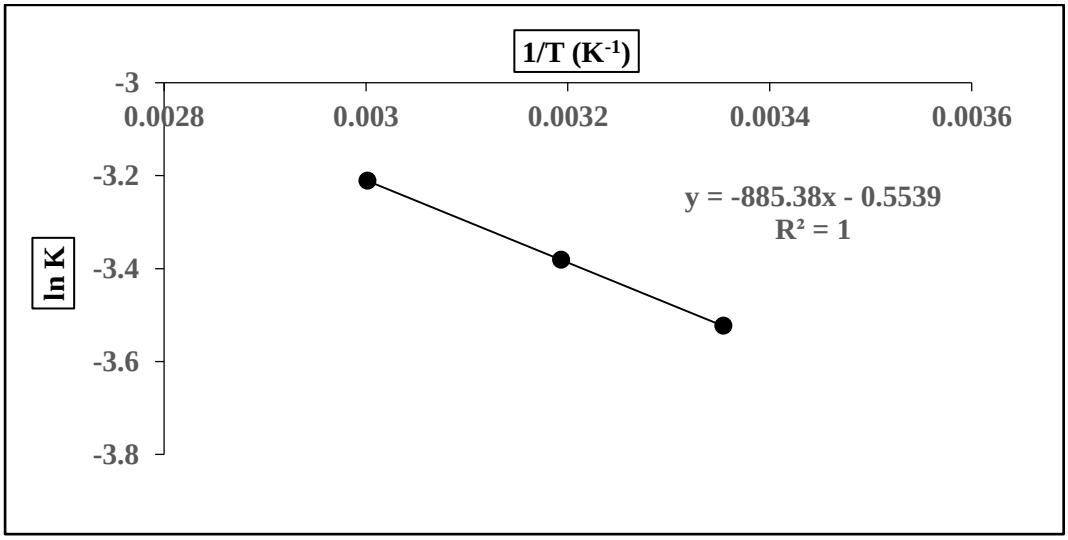

Figure (23): Plot (ln K vs. 1/T) for S adsorption onto (C/AC), pH=11, 200ppm, (25,40,60)^{0}C

Table 7: thermodynamic parameters for MB and S adsorption onto (C/AC), pH=11, 200ppm, (25,40,60) ^{0}C

E_a (KJ/mol)	ΔG (KJ/mol)	ΔS(KJ/mol/K)	ΔH (KJ/mol)	Temperature K	Adsorbent	Dyes
-6.2252	-4.5209	0.0352	5.9885	298.15	(C/AC)	**Methylene**

	-5.0496			313.15		**blue**
	-5.7546			333.15		
-7.3610	-2.5772	0.0473	11.5315	298.15	(C/AC)	**Safranine**
	-3.2870			313.15		
	-4.2334			333.15		

4. Conclusion

It is possible to prepare activated carbon derived from natural materials available at cheap prices and use it as adsorbent surfaces to remove hazardous dyes from the aqueous solutions. The adsorption capacity in terms pH of the solution, agitation time and temperature was examined. The control parameters were optimized and fixed. The isotherm investigation on adsorption of Methylene blue and Safranine onto activated carbon derived from cinnamon (C/AC) revealed best fit of Freundlich isotherm that indicated multilayer adsorption for MB and S onto the adsorbent surfaces. The kinetic studies confirmed pseudo-first order mechanism for adsorption system of MB and S. The thermodynamic studies indicate that the adsorption was spontaneous, endothermic and from E_a values indicate that the kind of adsorption was (physisorption). From all that we indicate that the prepared activated carbon surfaces could be used as adsorbents with high efficiency for removing contaminating dyes MB and S, and the adsorption efficiency depends on pH, time and temperature.

References

1. N. A. Youssef, S. A. Shaban, F. A. Ibrahim, A. S. Mahmoud. "Degradation of Methyl Orang using Fenton catalytic reaction, Egyptian Journal of Petroleum, (2016):25, (317-321).

2. B. K. Nandi, A. Goswami, M. K. Purkait. "Adsorption characteristics of Brilliant Green dye on kaolin", Journal of Hazardous Materials, (2009):161, (387-395).

3. G. K. Sarma, S. Sen Gupta, K. G. Bhattacharyya. "Removal of hazardous Basic Dyes from aqueous solution by adsorption onto Kaolinite and Acid-Treated Kaolinite: Kinetics, Isotherms and Mechanistic Study", Springer Natural Journal, (2019):1.

4. Z. Liu, K. Xing. "Removal of AcidRed88 using activated carbon produced from Pomelo Peels by KOH activation: Orthogonal Experiment, Isotherm and Kinetic studies", Hindawi Journal of Chemistry, (2021):2021.

5. F. Mashkoor, A. Naser. "Magsorbent: Potential Candidates in wastewater treatment technology – A review on the removal of Methylene Blue dye", Journal of Magnetism and Magnetic Materials, (2020):500, (166408).

6. S. Khamparia, D. Jaspal. "Investigation of adsorption of Rhodamine B onto natural adsorbent Argemone Mexican", Journal of Environmental Management, (2016):183, (786-793).

7. M. Vakili, M. Rafatuiiah, B. Salamatinia, M. H. Ibrahim, A. Z. Abdullah. "Elimination of Reactive Blue 4 from aqueous solution using 3 – Amino propyl Triethoxysilane modified Chitosan beads", Carbohydrate Polymers, (2015):132, (89 – 96).

8. M. Rajab, B. Mirza, K. Mahanpoor, M. Mirijalili, F. Najafi, O. Moradi. "Adsorption of Malachite Green from aqueous solution by Carboxylate group functionalized Multi – Walled carbon nanotubes: Determination of Equilibrium and Kinetics parameters", Journal of Industrial and Engineering Chemistry, (2015):34, (130-138).

9. K. A. Adegoke, O. S. Bello. "Dye sequestration using agricultural waste as adsorbents", Water Resources and Industry, (2015):12, (8 – 24).

10. M. Rafatullah, O. Sulaiman, R. Hashim, A. Shmad. "Adsorption of Methylene Blue on Low – Cost adsorbent: A review ", Journal of Hazardous Materials, (2010):177, (70 – 80).

11. R. G. Hunter, J. W. Day, A. R. Wiegman, R. R. Lane. "Municipal wastewater treatment costs with an emphasis on assimilation wetland in Louisiana Coastal Zone", Ecological Engineering, (2018);137, (21-25).

12. J. Fito, H. Said, S. Feleke, A. Worku. "Fluoride removal from aqueous solution onto activated carbon of Catha edulis through the adsorption treatment technology", Environmental System Research, (2019):8, (1-10).

13. L. S. Lima, M. D. M. Araujo, S. P. Quinaia, D. W. Miliorine, J. R. Garcia. "Adsorption modeling of Cr, Cd and Cu on activated carbon of different origins by using fractional factorial design", Chemistry Engineering Journal, (2011):166, (881 – 889).

14. S. D. Gisi, G. Lofrano, M. Grassi, M. Natarnicola. "Characteristics and adsorption of Low – Cost sorbents for wastewater treatment: a review", Sustainable Materials and Technologies, (2016):9, (10 – 40).

15. A. A. Abdulwahid, A. A. Alwattar, A. Haddad, M. Alshareef, J. Moore, S. G Yeates, P. Quayle." An efficient reusable perylene hydrogel for removing some toxic dyes from contaminated water", polym. Int. (2021):70, (1234 – 1245).

16. H. S. Al-Niaeem, A. A. Abdulwahid, W. Hanoosh, "Preparation of Semi IPNs-Hydrogel Composite for Removing Congo Red and Bismarck Brown Y from Wastewater: Kinetic and Thermodynamic Study", Egypt. J. Chem. (2022):65, (19 – 34).

17. M. Z. Ahmad, N. S. Afandi, K. A. Adegoke, O. S. Bello. "Optimization and batch studies on adsorption of Malachite Green dye using Rambuten Seed activated carbon", Desalination and water treatment, (2015):57, (2148-21511).

18. E. Aker, A. Altinisik, Y. Seki. "Using of activated carbon produced from spent Tea Leaves for the removal of Malachite Green from aqueous solution ", Ecological Engineering, (2013):52, (19 – 27).

19. O. S. Bello, M. A. Ahmad, B. Semire. "Scavenging Malachite Green dye from aqueous solution using Pomello (citrus grandis) peels: Kinetic, Equilibrium and Thermodynamic studies", Desalination and Water Treatment, (2015):56, (521-535).

20. D. Li, J. Yan, Z. Liu. "Adsorption kinetic studies for removal of Methylene Blue using activated carbon prepared from Sugar Beet Pulp", Journal of Environmental and Science Technology, (2016):13, (1815-1822).

21. M. Ahiduzzaman, A. K. M. Sadrul-Islam. "Preparation of porous and bio – char and activated carbon from Rice Husk by leaching ash and chemical activation", Springer Plus, (2016):5, (1248).

22. S. Vasanth, R. S. Gopel, S. Rekha, V. Srinivasan. "The in vitro antibacterial activity of Hedyotis Umbellata", Indian Journal of Pharmaceutical science, (2006):68, (236 – 238).

23. M. T. Samat. "A History of Food", Chichester, U.K., Ed.2end, (2009).

24. R. A. Mansour, A. Elshahawy, A. Attia, M. S. Beheary. "Brilliant Green dye biosorption using activated carbon derived from Guava Tree Wood", Hindawi International Journal of chemical Engineering, (2020):2020.

25. Z. Xu, T. Zhang, Z. Yuan, D. Zhang, Z.Sun, Y. Huang, W. Chen. "Fabrication of cotton textile waste – based magnetic activated carbon using $FeCl_3$ activation by

the Box – Behnken design: Optimization and Characteristics", The Royal Society of Chemistry, (2018), (38081 – 38090).

26. K-L. Chiu, D. H. L. Ng, "Synthesis and characterization of cotton-made activated carbon fiber and its adsorption of Methylene Blue in water treatment", Biomass and Bioenergy, (2012):46,(102 – 110),.

27. M. Elkody, H. Shokry, H. Hamad. "New activated carbon from Mine Cool for adsorption of dye in simulated water or multiple heavy metals in real wastewater", J. Materials, (2020):13, (2498).

28. D. Momodu, M. Madito, F. Barzeger, A. Bello, A. Khaleed, O. Olaniyan. "Activated carbon derived from tree bark biomass with promising material properties for super capacitors", J. Solid Electro chem, (2017):21, (859-872).

29. J. M. Al-Shawi, T. Z. Jassim, A. T. Al-Samarraie. Basra Journal Science, (2004).

30. H. S. Al-Niaeem, A. A. Abdulwahid, W. S. Hanoosh, "Removal of Carcinogenic Dyes Congo red (CR) and Bismarck brown Y (BBY) by Adsorption onto Reusable Hydrogels Derived from Acrylamide", Journal of Physics, (2021):2063, (1 – 28).

31. M. T. Uddin, M. A. Rahman, M. Rukanuzzaman, M. T. Islam. "Apotential low-cost adsorbent for removal of cationic dyes from aqueous solution ", Apple Water Sci, (2017):7, (2831-2842).

32. M. Zahid, N. Nadeem, N. Tahir, Farid-Un-Nisa, M. I. Majeed, Asim-Mansha. "Hybrid nanomaterials for water purification. In: Multifunctional Hybrid Nanomaterials for Sustainable Agri-Food and Ecosystems", Elsevier book, (2020), (155-188).

33. S. Sivaprakash, P. S. Kumar, S. K. Krishna, S. Sivaprakasha. "Adsorption study of various dyes on Activated Carbon Fe_3O_4 Magnetic Nano Composite", Int J. Apple Chem, (2017):13, (255 – 266).

34. N. K. Mondal, S. Kar, "Potentiality of banana peel for removal of Congo red dye from aqueous solution: Isotherm, kinetics and thermodynamics studies, Appl Water Sci, (2018):8, (157).

35. A. Djelad, A. Mokhtar, A. Khelifa, A. Bengueddach, and M. Sassi, “Alginate-whey an effective and green adsorbent for crystal violet removal: kinetic,

thermodynamic and mechanism studies," International Journal of Biological Macromolecules, (2019):139, (944 – 954).

36. M. Belhadri, A. Mokhtar, S. Meziani, F. Belkhadem, M. Sassi, and A. Bengueddach, "Novel low-cost adsorbent based on eco- nomically modified bentonite for lead (II) removal from aque- ous solutions," Arabian Journal of Geosciences, (2019):12, (88).

37. B. H. Hameed, "Removal of cationic dye from aqueous solution using jackfruit peel as non- conventional low-cost adsorbent," Journal of Hazardous Materials, (2009):162, (344 – 350).

38. S. Madhavakrishnan, K. Manickavasagam, K. Rasappan, P. S. S. Shabudeen, R. Venkatesh, and S. Pattabhi, "Ricinus communis pericarp activated carbon used as an adsorbent for the removal of Ni (II) from aqueous solution," E-Journal of Chemistry, (2008):5, (761 – 769).

39. N. Bouchikhi, M. Adjdir, K. C. Bendeddouche et al., "Enhance- ment of adsorption capacity of low cost mesoporous MCM-41 and their antibacterial and antifungal activities," Materials Research Express, (2019):6, (12507).

40. C. S. Betianu, P. Cozma, M. Rosca, E-D. C. Ungureanu, I. Mamaliga, M. Gavrilescu. "Sorbent of organic pollutants onto soils: Surface diffusion mechanism of Congo Red azo dye", Processes, (2020):4, (9 – 16).

41. M. A. Al-Ghouti, R. S. Al-Absi. "Mechanistic understanding of the adsorption and thermodynamic aspects of cationic Methylene Blue dye onto cellulosic Olive stones biomass from wastewater", Sci Rep. (2020):10, (1 – 40).

42. H. V. Tran, L. T. Hoang, C. D. Huynh. "An investigation on kinetic and thermodynamic parameters of Methylene Blue adsorption onto graphene-based nanocomposite, Chem Phys. (2020):535, (110793).

43. A. A. Mizhir, A. A. Abdulwahid, H. S. Al-Lami, "Chemical Functionalization Graphene Oxide for The Adsorption Behavior of Bismarck Brown Dye from Aqueous Solutions", Egypt J. Chem. (2020):63, (1679 – 1696).

44. M. T. Amin, A. A. Alazba, M. Shafiq. "Nonspontaneous and multilayer adsorption of Malachite Green dye by Acacia nilotica waste with dominance of physisorption", Water Sci Technol. (2017):76, (1805 – 1815).

45. N. Danesh, M. Ghorbani, A. Marjani. "Separation of copper ions by nanocomposite using adsorption process", Sci Rep. (2021):11, (1676).

46. A. A. Swelam, M. B. Awad, Y. R. Gedamy, A. Tawfik. "Fe_3O_4 nanoparticles: Synthesis, characterization and application in removal of iron aqueous solution and groundwater", Egypt J. Chem. (2019):62, (1189 – 1209).